ELSEVIER

Journal of Nuclear Materials 290–293 (2001) 753–756

journal of nuclear materials

www.elsevier.nl/locate/jnucmat

Particle simulation of detached plasma in the presence of diffusive particle loss and radiative energy loss

T. Takizuka [a,*], M. Hosokawa [b], K. Shimizu [a]

[a] *Japan Atomic Energy Research Institute, Naka Fusion Research Establishment, Naka, Ibaraki 311 0193, Japan*
[b] *Research Organization for Information Science and Technology, Tokai, Ibaraki 319 1106, Japan*

Abstract

The effect of diffusive particle loss and radiative energy loss on the formation of detached plasma is studied by using a particle simulation code PARASOL. The density near the divertor plate is decreased by the diffusion, and temperature is decreased by the radiation. The temperature drop does not make the density high, because of the generation of supersonic flow near the plate. The condition of the supersonic flow is $C \equiv (R_\Gamma/R_p)\sqrt{T_{\mathrm{plate}}/T_{\mathrm{throat}}} < 1$ (R_Γ: particle flux amplification factor; R_p: momentum flux reduction factor; T_{plate}: temperature at the plate; T_{throat}: temperature at the throat), and the Mach number at the plate is given as $M = C^{-1} + \sqrt{C^{-2} - 1}$, which is larger than unity. The simulation results agree well with this expression. The relation between diffusion/radiation and the detached plasma is discussed; low density due to the supersonic flow can bring about the detachment easily.

Keywords: Divertor plasma; SOL plasma; Detached plasma

1. Introduction

The divertor is expected to play key roles in tokamak reactors, such as ITER, for heat removal, ash exhaust, and impurity shielding. These divertor functions have been studied experimentally in many divertor tokamaks. Analyses of experimental results and extrapolation of the results to the divertor performance of future reactors are being carried out by using comprehensive simulation codes with the fluid model [1]. In the fluid model for scrape-off layer (SOL) and divertor plasmas, however, various physics models are introduced, i.e., boundary conditions at the plasma–wall boundary, heat conductivity, viscosity and so on. A kinetic approach is required to examine the validity of such physics models. One of the most powerful kinetic models is particle simulation [2,3]. A particle simulation code PARASOL (PARticle Advanced simulation for SOL and divertor plasmas) is used in the present study.

In order to reduce the heat load on divertor plates, the detached divertor plasma is a strong candidate for the operation of reactors. Because both particle and heat fluxes to the divertor plate decrease drastically in a detached plasma, the removal of plasma momentum as well as the removal of plasma energy near the plate is essential for the formation of detached plasma. Charge-exchange and recombination processes are considered to play important roles in momentum removal. Experimental observations on the detachment are reviewed in [4]. Theoretical considerations on this subject are given in [5,6]. The drift in SOL and divertor plasmas affects the condition of detachment. The PARASOL simulation shows that a detached plasma is formed in a divertor region where $E \times B$ drift with a speed exceeding a critical value flows out from the plate [7].

Particle diffusive loss can also remove the momentum efficiently. Although the qualitative condition for detached-plasma formation has been understood so far, the detailed mechanism and feature of the detachment have not fully been clarified yet. In the present study, we investigate the effects of diffusive particle loss and

* Corresponding author. Tel.: +81-29 270 7518; fax: +81-29 270 7419.

E-mail address: takizukt@fusion.naka.jaeri.go.jp (T. Takizuka).

0022-3115/01/$ - see front matter
PII: S 0 0 2 2 - 3 1 1 5 (0 0) 0 0 4 5 2 - 9

radiative energy loss on detached-plasma formation. Section 2 describes the model of PARASOL simulation. In Section 3, simulation results are shown. The effects of diffusive particle loss and radiative energy loss are studied. The generation of the supersonic flow is demonstrated there. The relation between diffusion/radiation and the detached plasma is discussed is Section 4, and conclusions are given in Section 5.

2. Simulation model

The PARASOL code is a modified and advanced code from the previous one described in [3]. The one dimensional (1D) system with a system length L is employed here. Two divertor plates are located at positions $x = -L/2$ and $L/2$. Both plate surfaces are perpendicular to the x direction, i.e., the x direction is normal to the plate. The magnetic field B is constant, and it intersects the divertor plates obliquely, i.e., the incident pitch of the magnetic field line $\Theta \equiv B_x/B < 1$.

The hot particle source is put in the central region of the SOL plasma, $-L_s/2 < x < L_s/2$. The schematic system is shown in Fig. 1. The cold particle source is put near the divertor plate, $L/2 - L_d < x < L/2$, which simulates the recycling source. Generated particles flow into divertor plates and vanish there. They are also lost from the system by cross-field diffusion. This diffusive loss is modeled as follows: in the diffusion region, $L/2 - L_d < x < L/2$ (the same as the cold-source region for the present study), a pair of an ion and an electron, whose separation distance is the minimum, is selected probabilistically to be lost. The diffusive loss then does not make a potential perturbation. A certain number of pairs are lost in a time step Δt. The ratio of the cold particle flux to the total particle flux, Γ_c/Γ_{tot}, and the ratio of the diffusive loss flux to the total flux, $\Gamma_{dif}/\Gamma_{tot}$, are input parameters. Radiative energy loss is simulated

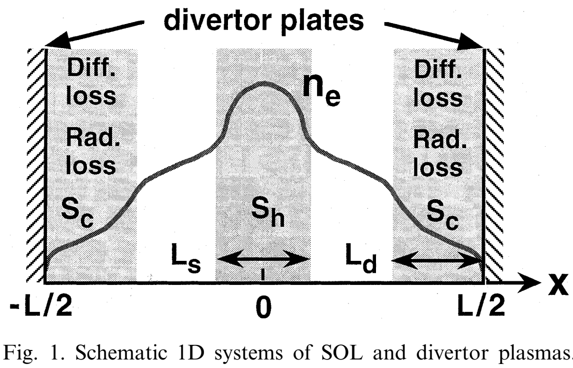

Fig. 1. Schematic 1D systems of SOL and divertor plasmas. Hot particle source (S_h) is put in the central region. Cold particle source (S_c), diffusive particle loss zone, and radiative energy loss zone are located near the divertor plate.

as follows: all electrons in the radiation region, $L/2 - L_d < x < L/2$ (the same as the cold-source/diffusion region for the present study), are decelerated keeping their velocity directions. The relative change in speed during Δt is the same for all electrons, and is much smaller than unity. The ratio of the radiative-energy-loss flux to the total energy flux, Q_r/Q_{tot}, is an input parameter.

Electron motions are approximated as their guiding-center motions (1D–2V), while ion motions are fully traced (1D–3V). The electrostatic field along the x direction is calculated with a usual PIC method. A radial electric field, E_r, which is perpendicular to the x-axis and the magnetic field, was given in our previous simulation study of the effect of $E \times B$ drift [7]. In the present work E_r is absent. The collisional effect is essential in the scrape-off layer plasma, and is simulated by a binary collision model [8]. The major procedures of the model are as follows: (1) In a time interval, a particle in a cell suffers binary collisions with an ion and an electron which are chosen randomly in the same cell. (2) Change in the relative velocity results from a coulomb interaction. Total momentum and total energy are conserved. This model describes the Landau collision integral.

The simulation parameters are as follows: As for the numerical parameters, the number of ions N_i is 10^5, the number of spatial grids M_x are 800, the grid size Δ_x is $\lambda_{D0}/2$ (λ_{D0}: Debye length at hot electron temperature T_{e0} and initial uniform density n_{e0}), and the time step Δt is ω_{p0}^{-1} (ω_{p0}: plasma frequency at n_{e0}). As for the physical parameters, the charge number of ions is unity, the mass ratio m_i/m_e is 400, the temperature ratio of hot source T_{i0}/T_{e0} is 1/2, the temperature of the cold source is 1/10 of the hot source temperature ($T_{ec}/T_{e0} = T_{ic}/T_{i0} = 1/10$), the width of the hot source region L_s is $0.2 \times L$, the width of the diffusion/radiation/cold-source region L_d is $0.2 \times L$, the incident pitch of the magnetic field Θ is 0.02, the collisionality $L_{\parallel}/l_{mfp0}$ is 2 ($L_{\parallel} \equiv L/\Theta$ :: system size along the magnetic field, and l_{mfp0}: mean free path at T_{e0} and n_{e0}), and the normalized Larmor radius ρ_{i0}/L is 0.004 (ρ_{i0}: ion Larmor radius at T_{i0}).

A simulation run continues to the time steps $K_t = 6 \times 10^4$, when the plasma becomes almost stationary. Results used for the present analysis are obtained from the averaged values during the last 10^3 time steps. A parallel computer Paragon XP/S15-256 is used for PARASOL simulations. The computation time of a run is about 8 h.

3. Results of PARASOL simulations

Simulation runs were performed in the parameter space ($\Gamma_{dif}/\Gamma_{tot}$, Γ_c/Γ_{tot}, Q_r/Q_{tot}) to study the effect of diffusion and radiation on the detachment. Fig. 2 shows the spatial profiles of SOL and divertor plasmas for

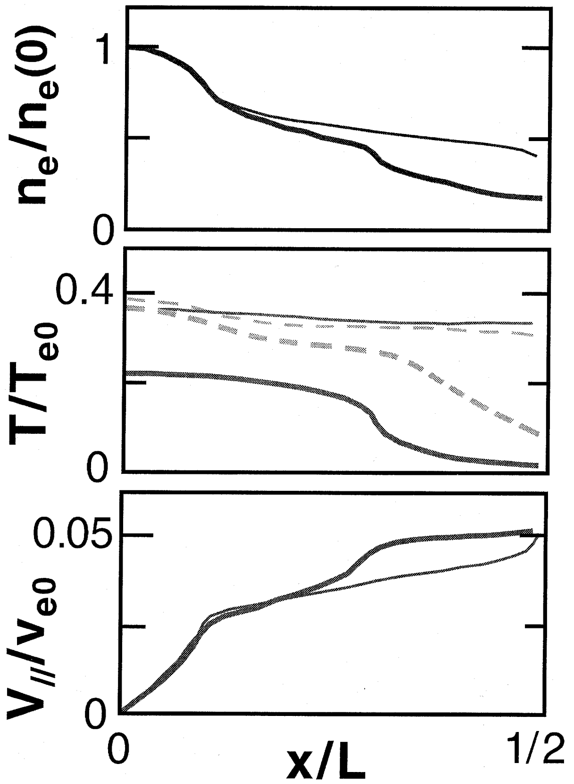

Fig. 2. Profiles of density, n_e, temperatures, T_e (solid line) and T_i (dashed line), and parallel flow velocity, $V_\parallel$. Thick lines correspond to the case of ($\Gamma_{dif}/\Gamma_{tot} = 0.5,\ Q_r/Q_{tot} = 0.6$) and thin lines, to the case of ($\Gamma_{dif}/\Gamma_{tot} = 0,\ Q_r/Q_{tot} = 0$).

($\Gamma_{dif}/\Gamma_{tot} = 0,\ Q_r/Q_{tot} = 0$) by thin lines, and for ($\Gamma_{dif}/\Gamma_{tot} = 0.5,\ Q_r/Q_{tot} = 0.6$) by thick lines. The flow velocity parallel to B, $V_\parallel$, is normalized by the electron thermal speed $v_{e0} = \sqrt{T_{e0}/m_e}$. The density and temperature are decreased near the divertor plate by the diffusion and radiation, while $V_\parallel$ is not decreased. We study how the density and temperature near the plate are changed by the diffusion and radiation. The ratio of n_d to $n(0)$ and the ratio of T_d to $T(0)$ are shown as functions of Q_r/Q_{tot} in Fig. 3(a) and of $\Gamma_{dif}/\Gamma_{tot}$ in Fig. 3(b), where $T = T_e + T_i$, suffix 'd' denoting a position near the divertor plate, and (0) denoting a central position. The temperature ratio $T_d/T(0)$ decreases with the increase of radiation loss, but the density ratio $n_d/n(0)$ is not affected by the radiation (Fig. 3(a)). On the other hand, $n_d/n(0)$ decreases with the increase of diffusion loss, but $T_d/T(0)$ is not changed by the diffusion (Fig. 3(b)). For large ($\Gamma_{dif}/\Gamma_{tot},\ Q_r/Q_{tot}$) values, the plasma pressure ($= n \times T$) near the plate becomes much lower than that at the center. If a simple assumption of $|V_\parallel| = C_s$ ($\equiv \sqrt{T/m_i}$: sound speed) in front of the plate is correct, the value of $n_d T_d$ is equal to $n(0)T(0)/2$ without diffusive loss. From Fig. 3(a), we find easily that this

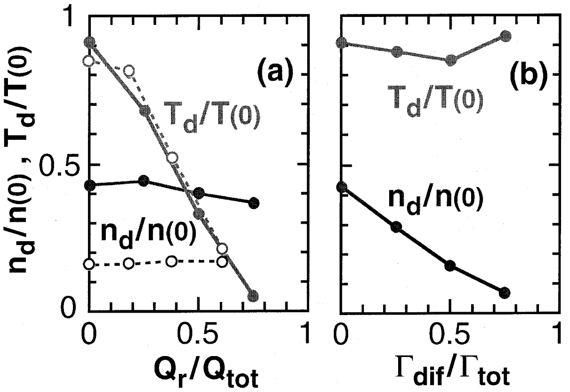

Fig. 3. Dependencies of density ratio $n_d/n(0)$ and temperature ratio $T_d/T(0)$ on Q_r/Q_{tot} (a) and $\Gamma_{dif}/\Gamma_{tot}$ (b). Suffix 'd' denotes position near the plate and (0) denotes central position. Solid lines in (a) are for $\Gamma_{dif}/\Gamma_{tot} = 0$ and dashed lines for $\Gamma_{dif}/\Gamma_{tot} = 0.5$.

simple assumption breaks, and the supersonic flow generates near the divertor plate: $|V_\parallel| > C_s$.

We consider the particle fluxes and momentum fluxes (effective pressure) at the divertor throat (suffix 1) and plate (suffix 2). Introducing a particle flux amplification factor R_Γ and a momentum flux reduction factor R_p, we obtain the following two relations,

$$n_2 M_2 \sqrt{T_2} = R_\Gamma n_1 M_1 \sqrt{T_1}, \tag{1}$$

$$(1 + M_2^2) n_2 T_2 = R_p (1 + M_1^2) n_1 T_1, \tag{2}$$

where $M \equiv |V_\parallel|/C_s$ denotes the Mach number. These equations are combined into an equation by eliminating n_1 and n_2,

$$(M_1 + M_1^{-1})/(M_2 + M_2^{-1}) = C \equiv (R_\Gamma/R_p)\sqrt{T_1/T_2}. \tag{3}$$

In addition to Eq. (3), the Bohm condition, $M_2 \geqslant 1$, is imposed. Solutions to Eq. (3) are given as follows:

$$M_2 \approx 1 \quad \text{and} \quad M_1 = C - \sqrt{C^2 - 1} \ \text{ for } C \geqslant 1, \tag{4}$$

$$M_1 \approx 1 \quad \text{and} \quad M_2 = C^{-1} + \sqrt{C^{-2} - 1} \ \text{ for } C \leqslant 1. \tag{5}$$

The case of $C \geqslant 1$ corresponds to high recycling, and the case of $C \leqslant 1$ to low recycling but high cooling. For the latter case, the supersonic flow generates near the plate ($M_2 > 1$). Fig. 4 shows the relation between M and C. The above solutions are drawn by a solid line (M_2) and by a dashed line (M_1). The results of PARASOL simulations with various values of ($\Gamma_{dif}/\Gamma_{tot},\ \Gamma_c/\Gamma_{tot},\ Q_r/Q_{tot}$) are plotted by closed circles (M_2) and open circles (M_1), which agree well with the analytical expressions.

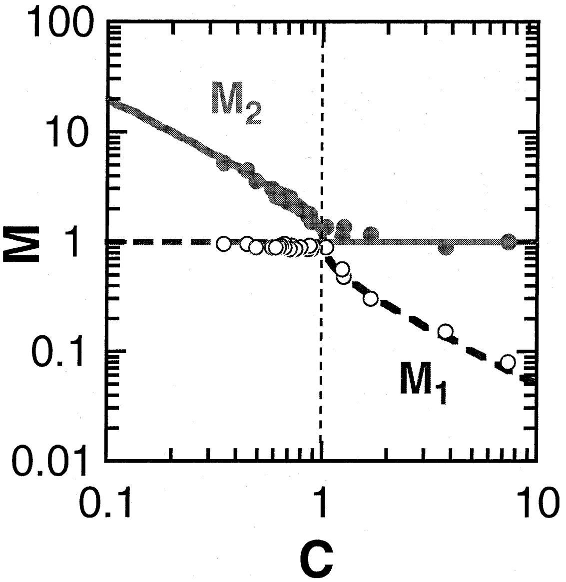

Fig. 4. Mach number M vs $C \equiv (R_\Gamma/R_p)\sqrt{T_2/T_1}$. Suffixes 1 and 2 correspond to throat and plate, respectively. Dashed line (M_1) and solid line (M_2) represent analytical solutions. Simulation results shown by circles agree well with analytical expressions.

4. Discussion

Here, we discuss the importance of the generation of supersonic flow. The possibility of supersonic flow was discussed in [5], but the importance of the supersonic flow was not pointed out. When the flow keeps subsonic, the density near the divertor plate can increase with the temperature decrease. High recycling state, then, can be maintained until the recombination process dominates. In the divertor region near the separatrix (hatched region in Fig. 5(a)), however, there exists a large diffusion loss due to the steep density gradient (Fig. 5(b)). The particle flux amplification along B, in this region, cannot become large compared with other divertor regions. When radiative cooling becomes strong in this region, the value of $C \equiv (R_\Gamma/R_p)\sqrt{T_1/T_2}$ can be reduced below unity. As a result, supersonic flow is generated and the density decreases. The density decrease makes the R_Γ value smaller, and this process is a positive feedback. We expect that the low density due to supersonic flow can bring about detachment easily in this region.

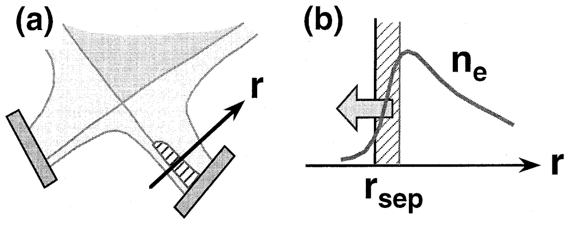

Fig. 5. Region expected to satisfy the condition $C < 1$ (hatched region) in radiatively cooled divertor plasma (a). Radial profile of density in this region (b). Large diffusion loss arises due to the steep gradient near the separatrix.

5. Conclusions

The effect of diffusive particle loss and radiative energy loss on the formation of detached plasma is studied by using a particle simulation code PARASOL. The density near the divertor plate is decreased by diffusion, and temperature is decreased by radiation. The temperature drop does not make the density high, because of the generation of supersonic flow near the plate. The condition of the supersonic flow is $C \equiv (R_\Gamma/R_p)\sqrt{T_{\text{plate}}/T_{\text{throat}}} < 1$, and the Mach number at the plate is given as $M = C^{-1} + \sqrt{C^{-2} - 1}$, which is larger than unity. The simulation results agree well with the analytical expressions. The relation between diffusion/radiation and the detached plasma is discussed; low density due to the supersonic flow can bring about detachment easily.

Two-dimensional particle simulation is planned to study the detached plasma. The 2D simulation includes naturally the $E \times B$ drift and the diamagnetic drift. We previously pointed out that the $E \times B$ drift induces the detachment [7]. The combined effects of supersonic flow and drift on the formation of detached plasma will be clarified in the near future. The interface between SOL plasma and detached plasma has not fully been understood so far. We will also show, in the near future, that a magnetic presheath plays an important role at the interface.

Acknowledgements

This work was performed under the Numerical EXperiment of Tokamak (NEXT) project in JAERI. The authors thank Drs T. Ozeki and Y. Kishimoto for their encouragement.

References

[1] T.D. Rognlien, B.J. Braams, D.A. Knoll, Contrib. Plasma Phys. 36 (1996) 105.
[2] R. Chodura, Phys. Fluids 25 (1982) 1628.
[3] T. Takizuka et al., J. Nucl. Mater. 128&129 (1984) 104.
[4] G.F. Mathews, J. Nucl. Mater. 220–222 (1995) 104.
[5] P.C. Stangeby, Nucl. Fus. 33 (1993) 1695.
[6] S.I. Krasheninnikov, Contrib. Plasma Phys. 36 (1996) 293.
[7] T. Takizuka, M. Hosokawa, Contrib. Plasma Phys. 40 (2000) 471.
[8] T. Takizuka, H. Abe, J. Comput. Phys. 25 (1977) 205.